Adv. Mater. App. 6 (2021) 6-15
ISSN: 2582-5070

Investigations on CdS reinforced PMMA Solid films of different molar concentrations for optical applications

S. Padmaja

Department of Physics, SRM Valliammai Engineering College, Kattankulathur-603203, Tamil Nadu, India

Corresponding author: padhdhu.sri2005@gmail.com.

Received 26 February 2021, Received in final form 27 March 2021, Accepted 27 March 2021

Abstract

A controlled and cost effective method of CdS:PMMA nanocomposite solid films have been prepared via insitu technique by controlling the flow of H_2S gas. PMMA was used as polymer capping without any additional chemical reagent to control the size of the CdS particles. The composition of CdS inside the polymer matrix was analyzed using X-ray photoelectron spectroscopy (XPS). UV-Visible spectrophotometer characterization shows the maximum transmittance of 92% for the composites. Differential scanning calorimetry (DSC) studies shows the thermal stability of the composites and the conductivity nature of the composites were studied using impedance analyzer

Keywords: *CdS:PMMA nanocomposite, Particle size distribution, Transmittance, Band gap.*

1. Introduction

Semiconducting nanocrystals, having size tunability, flexibility, low cost and easy fabrication technique have increased their demand and making them attractive materials for many applications such as light emitting diodes, lasers, sensors [1] and in solar cells [2]. Numerous materials and methods had been used to convert photon to electricity over the years and finally, semiconducting materials are found to be more promising [3]. Semiconductors, easily absorb photons when exposed to light. The light photon may excite the electron to higher levels and these electrons and holes, travel across the material by utilizing the electric field and finally can generate electrons through a load that can be used instantly or can be stored for future use. Besides, incorporating nanocrystals in polymer materials play a vital role in optical applications and preparation of hybrid organic/inorganic film has been done by the researchers [4,5]. But increasing the efficiency of the solar cells and to improve the light absorbing capacity of the materials for various applications are the challenge [6]. If their preparation method, and the semiconducting and polymer materials to be used for preparation have been chosen properly, it is possible to control the properties of the materials. The main challenge in preparing optical materials lies in its transparency, thickness, surface to volume ratio and controlling agglomeration of particles for reliability and sustainability.

Organic polymer materials reinforced with inorganic semiconducting materials, plays vital role in sensors [7], solar cells, lasers and LEDs. Organic materials are cost effective and will act as a good encapsulation for reinforced materials. Similarly, inorganic semiconducting materials are promising materials for optoelectronic devices and sensors. By varying the size of the semiconducting nanoparticles in polymer matrix, the band gap of the semiconductors can be tuned and in-turn, their absorption and emission spectra can be tailored for particular application. If the size of the semiconducting particle is reduced to the size of exciton (about 10 nm), the electronic and optical properties can be modified [8]. There have been several attempts to prepare free standing quantum dots. Because of their small size, nanoparticles have a very high surface to volume ratio resulting in a high reactivity and need to be stabilized [9]. When particles are not stabilized, they will generally undergo a process known as Ostwald Ripening [10]. To avoid this, researchers started preparing the semiconducting nanocomposites by reinforcing the semiconducting materials in polymer matrix along with organic ligand to restrict the particles from further growth. But this organic ligand is a barrier for transport of charge from nanoparticle to nanoparticle. The encapsulation of semiconductor particles in polymer matrix has the advantage of less loading with high polymer concentration. This is attributed to the much protected and capped

particles with the thick surrounding of polymer matrix. The solubility and dissolution of such polymer matrix based nanoparticles offers better possibility for their direct use in devices [11].

The solid state devices are highly preferred for optical applications such as optical limiters, semiconductor/polymer nanocomposite solar cells etc---Hence, the novelty of this work was the preparation of solid films of CdS:PMMA (Cadmium Sulphide:Poly(methylmethacrylate)) by simple and cost effective solution technique without any capping agent (organic ligand) other than the matrix polymer. The thickness of the solid films was very small. The CdS nanoparticles were prepared by insitu method and solid films were characterized for different studies.

2. Experimental method

Poly (methyl methacrylate) PMMA (M_w = $3.5x10^5$ g/m) and Cadmium nitrate $Cd(NO_3)_2.4H_2O$ were supplied by Aldrich and were used without any purification. PMMA was dissolved in 50 ml of Tetra hydro furan and stirred for 3 hours. After rigorous stirring, $Cd(NO_3)_2.4H_2O$ was added to the solution containing PMMA and stirred further for the complete dissolution of salt. In the initial stage, the concentrations were taken as 1:20, 1:60, 1:80 molar ratio. The formed films were dried in the ambient and the films were exposed to H_2S gas from Kipp's apparatus for half an hour. The films slowly changed from white to yellow which was the indication of the formation of CdS. Even the films formed out of higher concentration of CdS (1:20) were transparent and can be suitable for device applications. So the films having both higher concentration and lower concentration of CdS had been prepared and the concentrations had been extended to 1:100, 1:200 and 1:400 respectively. The device quality transparent solid yellow films of CdS: PMMA were obtained. The reaction mechanism for the formation of CdS particles in PMMA matrix was

$$Cd(NO_3)_2 + H_2S \rightarrow CdS + 2HNO_3\uparrow$$

The thickness of CdS:PMMA solid films were around 5 μm – 10 μm and was found using interferrometric technique.

3. Results and discussions

3.1 Compositional analysis

The XPS analysis have been carried out for CdS:PMMA composites to confirm the presence of CdS in the PMMA matrix and to verify the purity of the substance present in the matrix. Fig. 1 shows the XPS survey spectra of CdS:PMMA composites. The inset figures show the presence of Cd3d peaks and S_2P peaks.

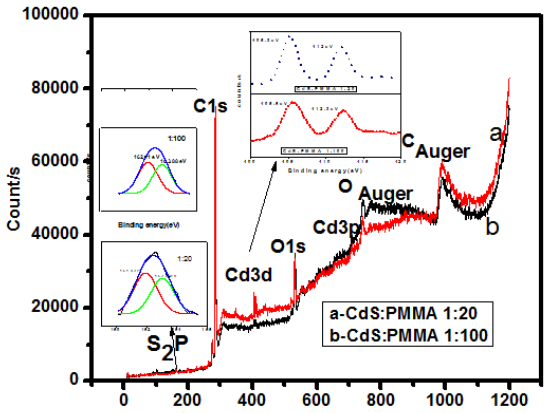

Fig. 1 *Survey spectra and Cd3d peaks, S_2P peaks (inset) of CdS:PMMA composites*

The survey spectra reveal the presence of C1s and O1s peaks. The C1s peak was deconvoluted into three components corresponding to C=O, C-C, and O-CH_3 which have originated from the PMMA matrix and were shown in figure 2a. Similarly, the O1s peak was deconvoluted and it gave three components, the C=O, C-O-C and H_2O and were shown in Figure 2b. The appearance of H_2O peak may be due to the slight absorbance of moisture by the solid films. The elements and their corresponding binding energies for C1s and O1s peaks were given in Table 1. For both the concentrations of CdS:PMMA (1:20 and 1:100), the presence of C1s and O1s peaks were at the same binding energy with negligible shift [12,13]. The Cd3d peaks observed for both the composites (Table 1) were in good agreement with the literature. Also the difference between the binding energies of $Cd3d^{5/2}$ and $Cd3d^{3/2}$ for both the concentrations was 6.7 eV which was in agreement with the literatures [14]. The S_2P peak positions present in both the concentrations of CdS:PMMA composites were shown in table 1.

Absence of sulphur peaks at 165 eV and 170 eV reveals the existence of sulphur in non- oxidized form. The shift in the binding energy of both Cd3d and S_2P sulphur peak for 1:100 CdS:PMMA concentration may attributed to the size effect of the particles [15] or the change in moiety.

3.2 Optical properties

3.2.1 UV-Visible absorption

The optical properties of CdS: PMMA composites were analysed using UV-Visible absorption spectra and transmittance spectra. The UV-visible absorption spectra of CdS:PMMA composites having

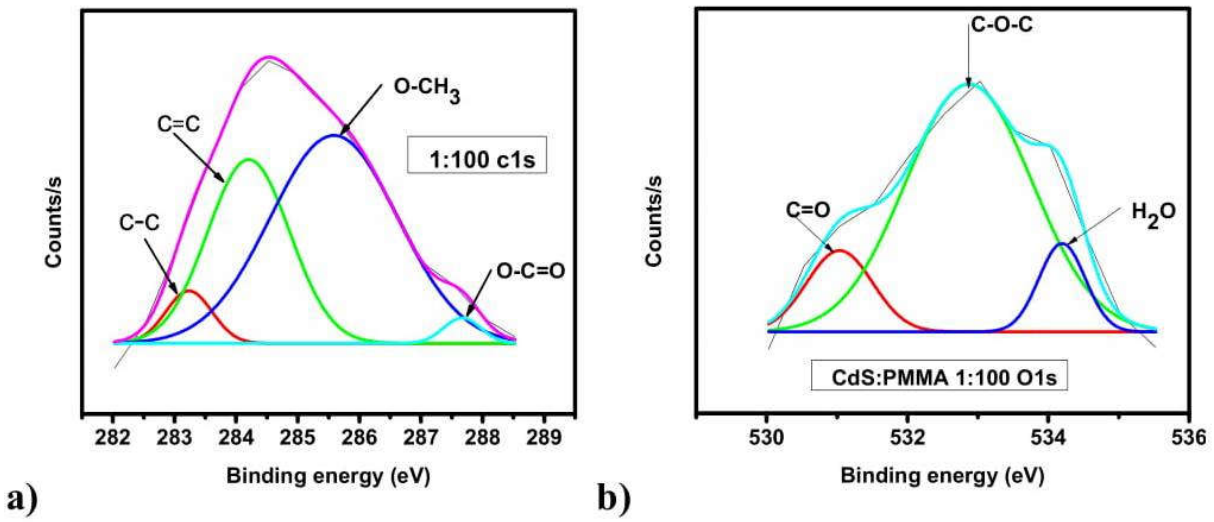

Fig. 2 *XPS spectra of C1s level and O1s level of CdS:PMMA composites (1:100)*

Table 1 *Binding energies of various elements of CdS:PMMA composites*

Composition (CdS:PMMA)	Elements	Binding energy(eV)	Composition (CdS:PMMA)	Elements	Binding energy(eV)
1:20	$Cd3d_{5/2}$	405.3	1:100	$Cd3d_{5/2}$	405.6
	$Cd3d_{3/2}$	412		$Cd3d_{3/2}$	412.3
	$S_2P_{3/2}$	162.41		$S_2P_{3/2}$	161.93
	$S_2P_{1/2}$	163.88		$S_2P_{1/2}$	163
	C1s (C-C)	283.2		C1s (C-C)	283.2
	C1s(C=C)	284.2		C1s(C=C)	284.4
	C1s($O-CH_3$)	285.5		C1s($O-CH_3$)	285.8
	C1s(-O-C=O)	287.6		C1s(-O-C=O)	286.4
	O1s(C=O)	531		O1s(C=O)	531.4
	O1s(C-O-C)	532.9		O1s(C-O-C)	532.9
	O1s(H_2O)	534.1		O1s(H_2O)	534.4

Table 2. *Transmittance of CdS:PMMA composites*

CdS:PMMA concentration	Transmittance (%)
1:20	85
1:100	90
1:200	90
1:400	92

the concentrations 1:20, 1:60,1:80 were shown in Figure 3. The absorption spectra shows obvious blue shift when compared to the bulk CdS onset which was around 515 nm (2.42eV) [16]. The absorption edges were measured by taking the intersection of the tangents drawn on the horizontal region between 500-600 nm and the inclined region between 400-500 nm of the curve. The absorption edges for the CdS:PMMA composites were 489, 442 and 436 nm for 1:20,1:60 and 1:80 concentrations respectively. The band edges were shifted towards blue region with decrease in concentration of CdS in PMMA matrix. There was only a small shift in the band edge values for CdS:PMMA composites of 1:60 and 1:80 concentrations. But the band edge values informed the CdS particle confinement in the PMMA matrix [17]. Hence the optical studies were carried out for both lower and higher concentrations (1:20,1:100, 1:200 and 1:400). The reported wavelength of absorption edge for bulk CdS was 515 nm [18] whereas for the prepared composites, the values of absorption band edges were 489, 419,410 and 409 nm respectively for films with CdS:PMMA concentrations 1:20, 1:100, 1:200 and 1:400 (not shown).

Table 3 *Emission wavelength of CdS:PMMA composites having different concentrations*

Concentration (CdS:PMMA)	Wavelength (nm) (lower energy)	Emission colour	Wavelength (nm) higher energy	Emission Colour
1:20	430	Blue	513,559	Green
1:100	415	Blue	521,567	Green
1:200	466	Blue	501,546	Green
1:400	406	Blue	428,454	Blue

Table 4 *Glass transition temperature at different concentrations of PMMA composites*

Concentration	Glass transition temperature $Cd(NO_3)_2$:PMMA (°C)	Glass transition temperature CdS:PMMA (°C)
Pure PMMA (112°C)	-	-
1:20	127	120
1:100	139	134
1:400	116	114

Table 5 *DC conductivity of PMMA composites before and after H_2S treatment*

Concentration of PMMA composites	dc conductivity (S/cm) (Before H_2S treatment)	dc conductivity (S/cm) (After H_2S treatment)
1:400	$2.1x10^{-12}$	$1x10^{-14}$
1:200	$2.17x10^{-12}$	$9.3x10^{-14}$
1:100	$2.2x10^{-13}$	$5x10^{-14}$
1:20	$2.7x10^{-12}$	$1.5x10^{-13}$

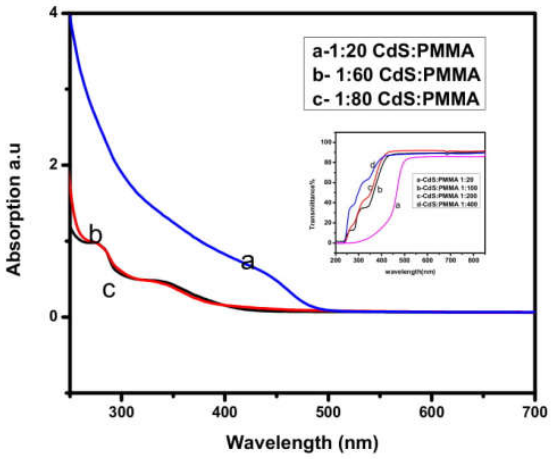

Fig. 3. *UV-Visible absorption spectra of CdS:PMMA composites. Inset-Transmittance spectra of CdS:PMMA composites.*

Fig. 3 inset shows the transmittance of CdS:PMMA composites. The optical transmittance was observed to shift towards shorter wavelength with decrease in CdS concentration for the composites. The small humps in the spectra were due to multimodal distribution of particles in the matrix. The spectra show good transmittance in the region above 500 nm which is one of the pre requisites for optoelectronic device applications [19,20]. Table 2 shows the maximum value of transmittance for 1:400 concentration as 92%. The results proved that the solid films of CdS:PMMA composites were highly transparent with minimum thickness.

The particle radii can be estimated from the band gap based on the models related to the size confinement effect (SCE). A model developed by Brus [21] for Effective mass Approximation (EMA) leads to the following equation:

$$E_{np} = E_{gb} + \frac{\hbar^2\pi^2}{2r^2}\left(\frac{1}{m_e^*} + \frac{1}{m_h^*}\right) - \frac{1.8e^2}{\varepsilon r} \qquad (1)$$

where E_{np} and E_{gb} are the respective nanoparticle and bulk energy gaps, r is the radius of the particle, $m_e^*(0.19m_0)$ & $m_h^*(0.8m_0)$ are the reduced masses of the conduction band electron and valence band hole in units of electron mass, h is Planck's constant ($4.1357x10^{-15}$ eV s), ε_o is the vacuum permittivity ($C^2\ J^{-1}\ M^{-1}$), ε is the dielectric constant (5.7 for CdS). The first term in Brus equation is referred to as the

quantum localization term (i.e. the kinetic energy term), which shifts the $E_g(r)$ to higher energies proportionally to r^{-2}. The second term in the Brus equation arises due to the screened coulomb interaction between the electron and hole, it shifts the $E_g(r)$ to lower energy as r^{-1}. The third term arises due to the Coulomb attraction between the electron and the hole.

CdS particle size for various CdS:PMMA concentrations were calculated using TBA model also. The best fit equation obtained for the empirical model (TBA) was as follows:

$$E_g = a_1 e^{-(d/b_1)} + a_2 e^{-(d/b_2)} \quad (2)$$

where the parameters a_1 and b_1 are 2.83 and 8.22, a_2 and b_2 are 1.96 and 18.07 and the expression was completely phenomenological.

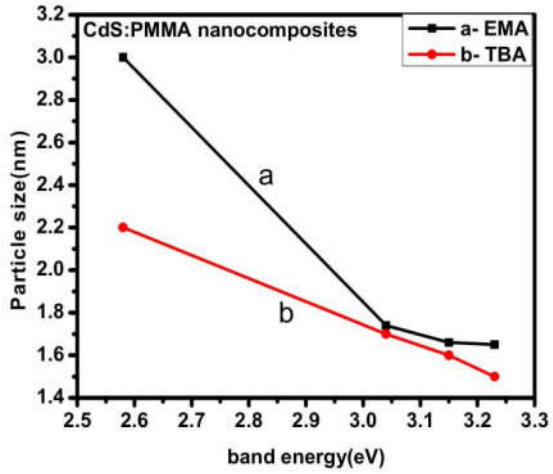

Fig. 4. *Particle size vs band energy of CdS:PMMA nanocomposites (a-EMA model b- TBA model)*

Fig. 4 shows the band energy vs particle size plot of CdS: PMMA nanocomposites. The particles sizes were calculated using both EMA model and TBA model. The confinement starts when the size of the particle is less than or equal to the Bohr radius of the atom. The Bohr radius of CdS is 3.5 nm [8]. In CdS:PMMA, the particle size was less than the Bohr radius of CdS and the particle was said to be in the strong confinement regime. However, the EMA model overestimates the particle sizes than TBA model. This may be due to the input parameters used for the calculation related to the bulk band gap [22]. But both the models reveal that the particles were in nanometer regime. Also, both the models are purely theoretical and it cannot be directly or indirectly compared with the experimental values of particle size

3.2.2 Luminescence nature

The room temperature photoluminescence (PL) spectra of CdS:PMMA nanocomposites had been recorded for the concentrations 1:20,1:100,1:200 and 1:400 respectively. The spectra were deconvoluted and were shown in Fig. 5. Table 3 illustrates that, in all the concentrations of CdS:PMMA, there was a peak in lower wavelength side which corresponds to near band edge emission of the nanocomposites (blue emission peaks) and the broad peak in the higher wavelength side corresponds to the surface trapped emission, dangling bonds, surface defects etc., which cannot be avoided in the composite preparations (green and blue emission) [23]. The peak maxima shifted towards blue region when the concentration of CdS:PMMA was reduced.

3.2.3 Size distribution

To perceive the distribution of CdS particles in PMMA matrix, the tapping mode AFM was used to characterize the nanocomposite solid films. Figure 6(i) shows the AFM image of pure PMMA solid film. The figure shows the presence of small spherical shaped holes throughout the films which was the indication of highly amorphous nature of PMMA polymer [24]. Figure 6ii)a, 6iii) a and 6iv) a shows the presence of uniformly distributed particles in amorphous polymer background. As the concentration of CdS particles in the PMMA matrix was high (1:20), the image appears to be occupied with denser particles. The height profile (6ii)b,6 iii) b and 6iv)b) shows the poly dispersed particles in the matrix for all the concentrations. The particle size distribution plot shows the minimum of 21 nm for 1:400 concentration (6 iv) c.) It reveals that, by decreasing the concentration of CdS in the PMMA matrix, the minimum particle size can be obtained. Conversely, the mean particle diameter was 35 nm in 1:100 CdS:PMMA concentration(Fig. 6 iii) c). Nayan Mani Das (2013) and his co-workers [25] have explained the random walking behaviour of CdS nanoparticles after H_2S treatment. The CdS nanoparticles in the PMMA matrix diffused through some distance called 'random walking' before they coalesce and after some time they form the heap of nanoparticles. So, the particle diameter seems to be large in 1:100 concentrations.

3.2.4 Thermal behavior

In order to study the thermal stability of CdS:PMMA nanocomposite solid films, the DSC measurements have been carried out. Since, PMMA is an amorphous polymer, the glass transition temp-

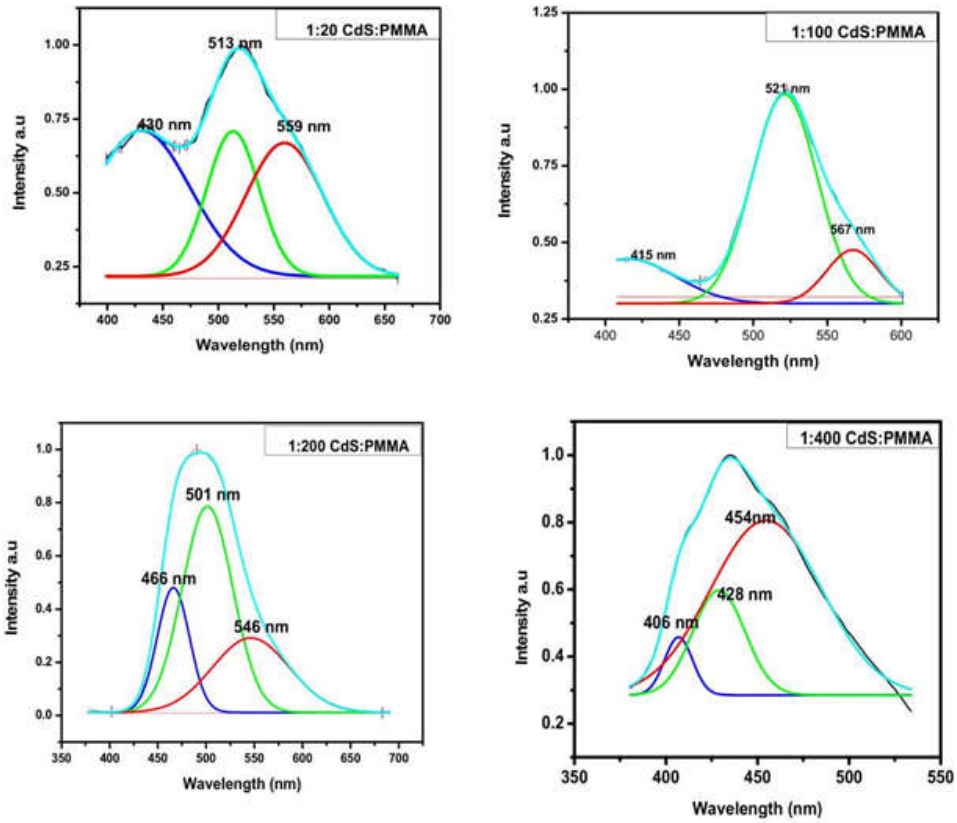

Fig. 5. *Deconvoluted PL spectra of CdS:PMMA nanocomposites*

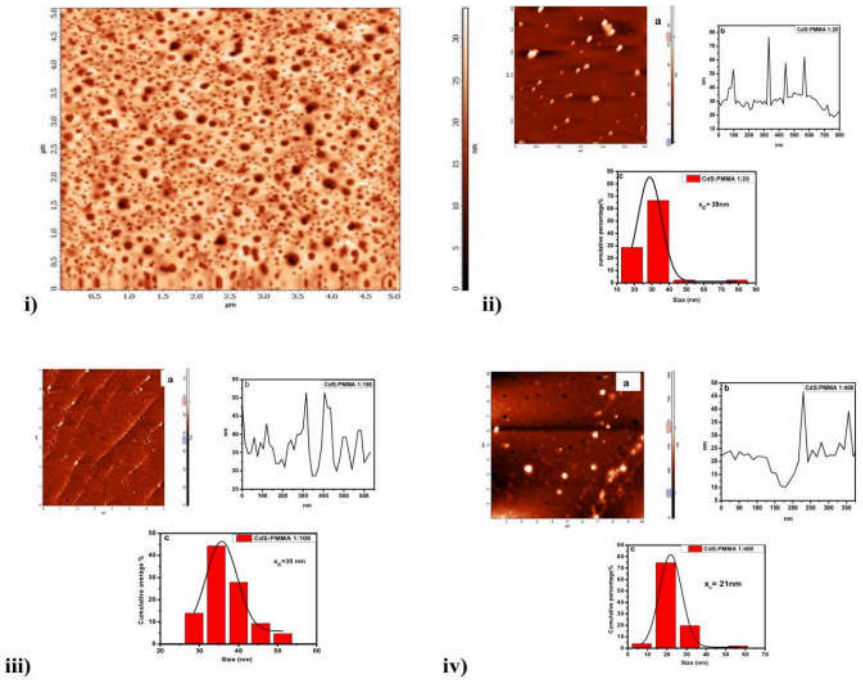

Fig. 6 *AFM images of i) pure PMMA ii) CdS:PMMA (1:20) iii) CdS:PMMA(1:100) iv) CdS:PMMA (1:400)*

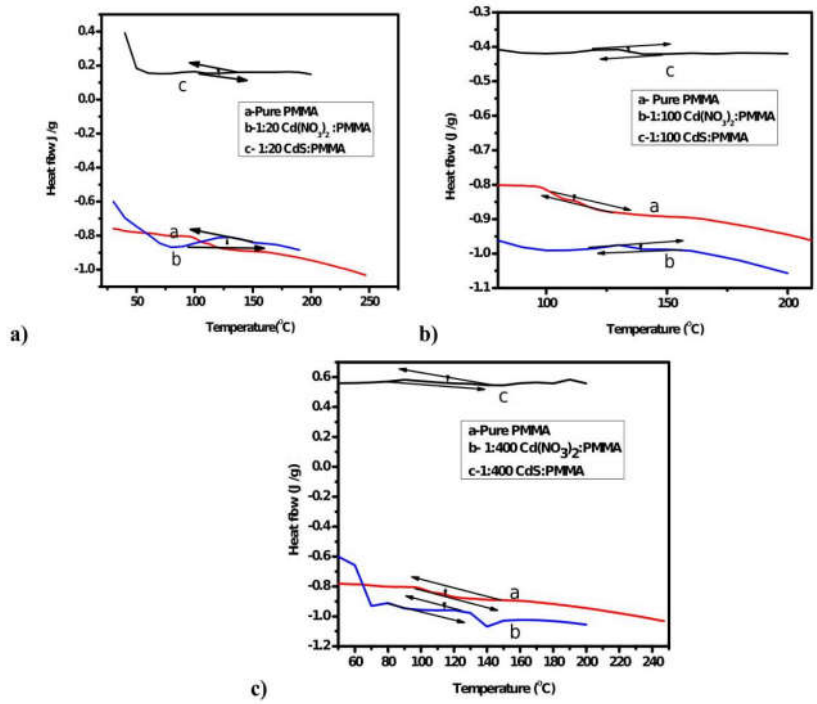

Fig. 7. *DSC thermogram of pure PMMA, $Cd(NO_3)_2$:PMMA and CdS:PMMA with different concentrations.*

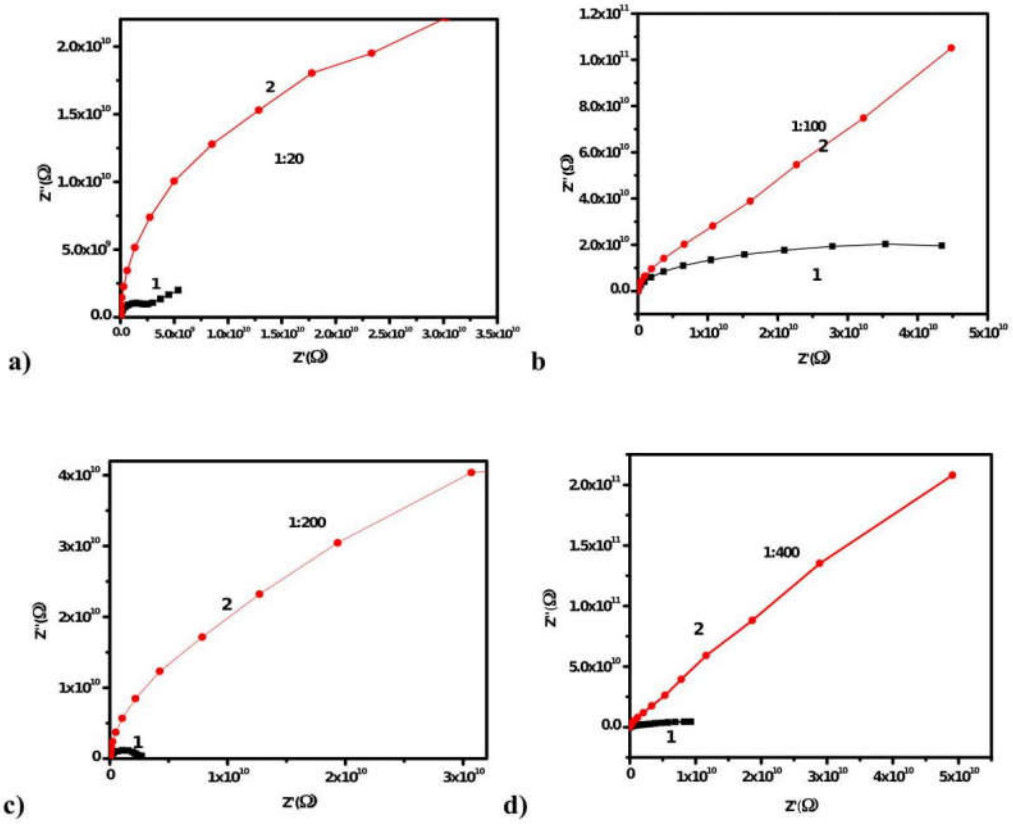

Fig. 8 *Impedance cole-cole plot for composites before and after H_2S gas treatment*

-erature of pure PMMA solid film was found to be around 112°C (taken in the mid of the slope) [26].

Fig. 7 show the DSC thermograms of pure PMMA solid film, $Cd(NO_3)_2$:PMMA (before H_2S treatment) and CdS:PMMA nanocomposite solid films having different concentrations (1:20,1:100 and 1:400). The glass transition temperature of all the concentrations before and after H_2S treatment was given in Table 4. The glass transition temperature of all the composites of different concentrations was higher than that of pure PMMA. The same trend was observed in the case of CdS:PMMA nanocomposite also. The shift in glass transition temperature of PMMA towards higher temperature was attributed to the incorporated Cd^{2+} ions as well as the CdS particles [27]. In the presence of Cd^{2+} ions, the free volume of the amorphous PMMA decreases and the segmental motion of the polymer chains were restricted by the Cd^{2+} ions. So the composite becomes hard and the glass transition temperature increases in all the composites before H_2S treatment. When the material was exposed to H_2S gas, the glass transition temperature slightly decreases but it was higher than the glass transition temperature of pure PMMA. After H_2S treatment, the random motion of the Cd^{2+} ions disappear and the CdS particles gets in to the voids present in the amorphous PMMA matrix and settle down in the matrix. Hence the free volume of the matrix decreases.

On the other hand, the increase in polymer-particle interaction reduces the mobility of polymer segments and increases the glass transition temperature of CdS:PMMA in 1:100 than 1:20. Again, when the concentration of CdS was less in 1:400, the increase in polymer-polymer interaction than the particle polymer interaction reduces the glass transition temperature [28]. The above results suggest that the thermal stability of the CdS:PMMA nanocomposites were superior to that of pure PMMA.

3.2.5 Electrical studies

The electrical studies were carried out using impedance analyzer for the samples before and after exposure treatment of H_2S gas. The studies were carried out in room temperature at the frequency range 0.001Hz to 1MHz. The bulk resistance (R_b) of the composites before and after H_2S treatment can be determined using the cole-cole plots from the intercept of the plot with the real axis. Fig. 8 shows the cole- cole (Nyquist) plots of different concentrations of PMMA composites before and after H_2S treatment. The plot displays the semicircular pattern in the high frequency range for all the composites before H_2S treatment followed by a spike (tail) in the low frequency region. The high frequency semicircle indicates the bulk properties of the material whereas the low frequency tail represents the capacitive nature of the material [29].

On the other hand, the disappearance of semicircle is observed in the case of CdS:PMMA nanocomposites. The steep spike in the low frequency region suggests the greater accumulation of charge carriers at electrode – electrode interface. Also it suggests the increase in the capacitive nature of the CdS:PMMA nanocomposites.

The dc conductivity of the samples can be calculated using the relation:

$$\sigma_{dc} = \frac{l}{R_b A} \quad (3)$$

Where 'l' is the thickness of the sample. 'A' is the electrode area of the sample and R_b is the bulk resistance of the sample [30]. The calculated dc conductivity was given in Table 5. The maximum dc conductivity for PMMA composites before and after H_2S treatment was obtained for 1:20 concentration. The results suggests that the high concentration of CdS in PMMA matrix is preferable for electrical applications. The overall room temperature dc conductivity of the CdS:PMMA nanocomposites was less than the reported dc conductivity of pure PMMA(10^{-11} S/cm) [29] . Further studies at various temperatures are required to show the better dc conductivity for CdS:PMMA nanocomposites.

4. Conclusions

We have presented the successful fabrication of CdS:PMMA nanocomposite solid films for optoelectronic applications. Various molar concentrations of CdS:PMMA nanocomposites were prepared. The XPS studies shows that the binding energies of various concentrations of the composites were in agreement with the literature. The band edges of the composites were shifted towards blue region with decrease in concentration of CdS in PMMA matrix. Also, the maximum transmittance of 92% was observed for lowest concentration of CdS in PMMA. The green emission is obtained for the composites by decreasing the concentration of CdS in PMMA matrix. The afore mentioned things reveals that the band gap and luminescence nature of the CdS:PMMA nanocomposites are tunable. AFM images exposed the uniform distribution of particles in the matrix and the average particle size vary with respect to the molar concentration of CdS:PMMA composites. DSC studies suggested the superior thermal stability of the composites compared to

pure PMMA. The maximum dc conductivity obtained for CdS:PMMA nanocomposites was around 1.5 $x10^{-13}$. The appearance of the cole-cole plots shows the increase in capacitive nature of the CdS:PMMA nanocomposites.

References:

[1]. Akanksha Mwhto, Varsha R Mehto, Jyotsana Chauhan, I. B. Singh, P. K. Pandey, "Preparation and characterization of polyaniline/ZnO composite sensor", J. Nanomed. Res. 5 (2017) 1-8.

[2]. D. Hernandez Martinez, M. E. Nicho, Hailin Hu, U. Leon-Silva, M. C. Arenas-Arrocena, C. H. Garcia Escobar, "Electrospinning of P3HT-PEO-CdS fibers by solution method and their properties", Mater. Sci. Semicond. Process. 61 (2017) 50-56.

[3]. Christoph Hellmann, Francis Paquin, Neil D. Treat, Annalisa Bruno, Luke X. Reynolds, Saif A. HAque, Paul N. Stavrinou, Carlos Silva, Natalie Stingelin, "Controlling the interaction of light with polymer semiconductors", Adv. Mater. 25 (2013) 4906-4911.

[4]. M. Bashouti, W. Salalha, M. Brumer, E. Zussman, E. Lifshitz, "Alignment of colloidal CdS nanowires embedded in polymer nanofibers by electrospinning", Chem. Phys. Chem. 7 (2006) 102-106.

[5]. Ryan Kissalinger, Weidi Hua, K. Arthik Shankar, "Bulk heterojunction solar cells based on blends of conjucated polymers with II-VI and IV-VI inorganic semiconductor quantum dots", Polymers 9 (2017) 1-29.

[6]. Martin A. Green, Keith Emery, Yoshihiro Hishikawa, Wihelm Warta, Ewan D. Dunlop, Dean H. Levi, Anita W. Y. Ho-Baillie, "Solar cell efficiency tables (Version 48)", Prog. Photovoltaic Res. Appl. 23 (2015) 1-9.

[7]. K. A. Sablon, "Polymer single-nanowire optical sensors", Nanoscale Res. Lett. 4 (2008) 94-95.

[8]. E. O. Chukwuocha, M. C. Onyeaju, "Simulation of quantum dots (QDs) in the confinement regime", Int. J. Appl. Sci. Eng. 1 (2012) 784-792.

[9]. Jingyu Shi (2002) "Steric stabilization", Ohio State University, USA.

[10]. Sang II Jeon, D. Joseph, Andrade, "The Steric repulsion properties of Poly(ethylene Oxide)", Bull. Korean. Chem. Soc. 13 (1992) 245-248.

[11]. Elizabeth Alice Thomsen (2008) "Characterisation of materials for organic photovoltaics", Ph.D thesis, University of St. Andrews. Scotland.

[12]. H. L. Pushpalatha, R. Ganesha, "X-ray photoelectron spectroscopic studies of CdS semiconductor thin films deposited by photochemical deposition", Int. J. Chem. tech. Res. 7(2015) 2171-2175.

[13]. W. Scott, Rocencrance, K. Wayne Way, Nicolas Winograd, David A Sirley, Polymethylmethacrylate by XPS, Surf. Sci. Spectra 2 (1993) 71-73.

[14]. N. Lakshmana Reddy, V. N. Avakoteseara Rao, M. Mamatha Kumari, P. Ravi, M. Sathish, M. V. Shankar, "Effective shutting of photo excitons on CdS/NiO core/shell photocatalysts for enhanced photocatalytic hydrogen production", Mater. Res. Bull. 101 (2018) 223-231.

[15]. V. L. Colvin, A. N. Goldstein, A. P. Alivisato, "Semiconductor Nanocrystals Covalently Bound to Metal Surfaces with Self-Assembled Monolayers", J. Am. Chem. Soc. 114 (1992) 5221-5230.

[16]. Li chen, Jia Zhu, Qing Li, Su Chen, Yanru Wang, "Controllable synthesis of functionalized CdS nanocyrstals and CdS/PMMA nanocomposite hybrids", Eur. Polym. J. 43 (2007) 4593-4601.

[17]. S. A. Filonovich, Yu. P. Rakovich, A. G. Rolo, M. V Artemyev, G. Hungerford, M. I. Vasilevskiy, M. J. M. Gomes, J. F. A. Ferreria, "Enhancement of photoluminescence intensity of CdS(Se) nanocrystal thin films", J. Optoelectron. Adv. Mater. 2 (2000) 623-628.

[18]. J. Gonzalez, Santiago-Jacinto, E. Reguera, "Controlled growth of CdS quantum dots", Sci. Adv. Mater. 1 (2009) 69-76.

[19]. Ruby Das , Suman Pandey, "Comparison of Optical Properties of Bulk and Nano Crystalline Thin Films of CdS using Different Precursors", Int. J. Mater. Sci. 1(2011) 35-40.

[20]. D. K. Dwivedi, Dayashankar, Maheshwar Dubey, "Synthesis, structural and optical characterization of CdS nanoparticles", J. Ovonic Res. 6 (2010) 57-62.

[21]. L. E. Brus, "Electronic wave functions in semiconductor clusters: experiment and theory', J. Phys. Chem. A 90 (1986) 2555-2560.

[22]. P. Nandakumar, C. Vijayan, K. Dhanalakshmi, G. Sundararajan, P. Kesavan Nair, Y. V. G. S. Murti, "Synthesis and characterization of CdS nanocrystals in a perfluorinated ionomer (Nafion)", Mater. Sci. Eng. B 83 (2001) 61-65.

[23]. M. Thambidurai, N. Muragan, N. Muthukumarawamy, R. Vasantha, R. Balasundaraprabhu, S. Agilan, "Preparation and characterization of nanocrystalline CdS thin films", Chalcogenide Lett. 6 (2009) 171-179.

[24]. Hanhong Li, Guangzhao Mao , K. Y. Simon Ng, "AFM study of template growth of Cadmium sulphide nanoparticles using pure and mixed

arachidate films", Thin solid films 358 (2000) 62-72,
[25]. Nayan Mani Das, Dhrubojyoti Roy, P. S Gupta, "Diffusion mediated agglomeration of CdS nanoparticles via Langmuir–Blodgett technique", Mater. Res. Bull. 48 (2013) 4223-4229.
[26]. Mohammad A. Aldosari, Ali A. Othman , Edreese H. Alsharaeh, "Synthesis and Characterization of the in Situ bulk Polymerization of PMMA Containing Graphene Sheets Using Microwave Irradiation", Molecules 18 (2013) 3152-3167.
[27]. Liyun Ding, Tao Li, Yunmin Zhong, Chao Fan, Jun Huang, "Synthesis and characterization of a novel nitric oxide fluorescent probe CdS-pmma nanocomposite via in-situ bulk polymerization", Mater. Sci. Eng. C 35 (2014) 29-35.
[28]. D. Patidar, Sonalika Agrawal , N. S. Saxena, "Glass transition activation energy of CdS/PMMA nano-composite and its dependence on composition of CdS nano-particles", J. Therm. Anal. Calorim. 106 (2011) 921-925.
[29]. Tan kia wui (2013) "Studies on the properties of pmma-based polymer electrolyte for lithium rechargeable battery", Ph.D Thesis, University of Tunku Abdur Rahman, Malaysia.
[30]. Mayank Pandey, M. Girish, Joshi, Kalim Deshmukh, Jamil Ahmad, "Impedence spectroscopy and conductivity studies of $Cdcl_2$ doped polymer electrolyte", Adv. Mater. Lett. 6 (2015) 165-171.

